

## 400 GHz 1.3 dBi Leaky Wave Antenna in CMOS 1.3 $\mu\text{m}$ Process

Qianru Weng\*, Xinru Li, Hsien-Shun Wu, and Ching-Kuang Tzuang

**Abstract**—A 400 GHz monolithic leaky wave antenna (LWA) is presented in this paper. The proposed LWA, constructed by the unit cell with multiple structural parameters, is regarded as the on-chip microstrip with perforation on the signal trace and the ground plane. A hybrid full-wave eigenvalue method theoretically extracts the complex propagation constants of first higher-order mode ( $\text{EH}_1$ ) of the perforated microstrip to improve the unit cell design. The extracted results also assist in realizing the differential feeding network to excite the leaky mode of the proposed antenna in high efficiency. A 400 GHz LWA prototype is designed and fabricated in CMOS 0.13  $\mu\text{m}$  1P8M process. The on-chip experiments show the measured input return loss including the effects of the contact pad lower than 10 dB from 380 GHz to 420 GHz. The measured antenna gain is higher than 0.8 dBi and has a maximum value of 1.3 dBi at 400 GHz. From 390 GHz to 405 GHz, the measured main beam is at  $33^\circ$  to  $43^\circ$  from broadside, indicating good agreement with the calculated results.

### 1. INTRODUCTION

Monolithic antennas, directly integrated into the radio frequency (RF) system-on-chip (SOC), become a promising technology to implement the wireless communication system over 100 GHz [1–3]. The on-chip antenna can be attached to the back of the quasi-optical lens to couple the electromagnetic energy into the lens through the monolithic substrate [2, 3] or directly radiates the electromagnetic energy from the top surface of the chip into free space [4, 5]. The monolithic resonating-type antennas, including the half-wavelength dipole [4], the patch antenna [5], and the slotted cavity [7] are reported. However, the theoretical estimations by using the curve in Fig. 6 of [8] with a thickness of 5.7  $\mu\text{m}$  between the signal and the ground, show the radiation efficiency of a patch antenna in the typical CMOS process is lower than 10%. The CMOS traveling wave antenna, so-called the leaky wave antenna (LWA) was reported to theoretically demonstrate its feasibility at 410 GHz [11]. In this paper, the rigorous hybrid eigenvalue approach presented in Section 2 is applied to improve the monolithic LWA design. The extracted complex propagation constants of the leaky mode reported in Section 3 lead to design the unit cell of the LWA with the significant reduction in the conductor loss. Additionally, the on-chip differential feeding network, instead of the asymmetrical matching network in [11], is designed to excite the leaky mode in high efficiency. The simulated antenna gain and efficiency is 2.8 dBi and 41.1% at 400 GHz. The on-chip experiments, which are reported in Section 4, show the measured antenna gain is 0.8 dBi from 390 GHz to 405 GHz and has a maximum value of 1.3 dBi at 400 GHz. The measured main-beam positions, having excellent agreements with the calculated results, are 30, 41, 45 and 51 degrees from broadside at 390, 400, 405, and 415 GHz. Section 5 concludes the paper.

### 2. CMOS LEAKY WAVE ANTENNA (LWA) INCORPORATING THE PERFORATED MICROSTRIP

Figure 1 shows the leaky wave antenna (LWA) implemented by using the perforated microstrip in the standard CMOS process. The top metal (M8) realizes the signal trace of the antenna. M1 metal-layer combines with M2 metal-layer to construct the antenna's ground plane. The substrate thickness,

---

Received 14 September 2016, Accepted 8 November 2016, Scheduled 23 November 2016

\* Corresponding author: Qianru Weng (wengqianru@tju.edu.cn).

The authors are with the School of Electronic Information Engineering, Tianjin University, Tianjin 300072, China.

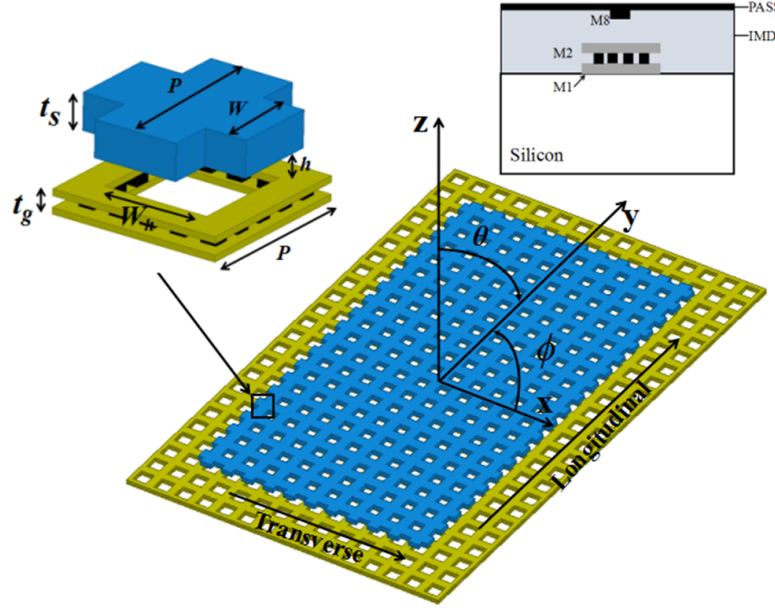


**Figure 1.** CMOS leaky-mode antenna: The substrate thickness ( $h$ ):  $5.7 \mu\text{m}$ , the permittivity ( $\epsilon_r$ ) of the substrate: 4, the thickness of ground plane ( $t_g$ ):  $2.0 \mu\text{m}$ , the thickness of signal trace ( $t_s$ ):  $3.3 \mu\text{m}$ , the conductivities of the signal trace and ground plane are  $5.82 \times 10^7$ , and  $4.61 \times 10^7 \text{ S/m}$ .

denoted by  $h$ , is equal to the distance between the M8 and M2 metal-layer. The perforated microstrip is made by the unit cell whose dimension is much smaller than the guiding wavelength at the operating frequency of the antenna. The five structural parameters, including the periodicity ( $P$ ), the mesh area of the ground plane ( $W_h$ ), the width of the connecting arm ( $W$ ), and the metal thicknesses of the signal trace and the ground plane ( $t_s$  and  $t_g$ ) define the unit cell to realize the monolithic LWA.

As shown in Fig. 1, the LWA consists of the periodical unit cells along the transverse and longitudinal directions. To extract the dispersion characteristics of the LWA, the numerical procedures based on the hybrid full-wave eigenvalue method are performed [12]. The perforated microstrip in Fig. 1 can be equivalently represented by the multiport network shown in Fig. 2. The unit cell duplicates  $M$  times along transverse direction and  $N$  times along longitudinal direction to form a  $M \times N$  array. In the reference plane 1 and 2, total  $M$  ports can be defined. The  $2M$ -port scattering parameters of the network in Fig. 2 can be obtained by using the commercial full-wave simulator ANSYS<sup>TM</sup> HFSS. Then, by converting the scattering matrix into ABCD matrix, the equivalent network in Fig. 2 can be represented by

$$\begin{bmatrix} a^{(1)} \\ \tilde{b}^{(1)} \\ \sim \end{bmatrix} = \begin{bmatrix} T & T \\ \approx_{11} & \approx_{12} \\ T & T \\ \approx_{21} & \approx_{22} \end{bmatrix} \begin{bmatrix} b^{(2)} \\ a^{(2)} \\ \sim \end{bmatrix} = \begin{bmatrix} T & T \\ \approx_{11} & \approx_{12} \\ T & T \\ \approx_{21} & \approx_{22} \end{bmatrix} \cdot e^{-\gamma \cdot N \cdot P - j(2n\pi)} \cdot \begin{bmatrix} a^{(1)} \\ \tilde{b}^{(1)} \\ \sim \end{bmatrix} \quad (1)$$

where  $P$  and  $N$  represent the periodicity and number of the unit cell in the longitudinal direction. Rearranging Eq. (1), the eigenvalue equation of the equivalent network in Fig. 2 is

$$\begin{bmatrix} T & T \\ \approx_{11} & \approx_{12} \\ T & T \\ \approx_{21} & \approx_{22} \end{bmatrix} \begin{bmatrix} a^{(1)} \\ \tilde{b}^{(1)} \\ \sim \end{bmatrix} = e^{\gamma \cdot N \cdot P + j(2n\pi)} \cdot \begin{bmatrix} a^{(1)} \\ \tilde{b}^{(1)} \\ \sim \end{bmatrix} = \lambda \cdot \begin{bmatrix} a^{(1)} \\ \tilde{b}^{(1)} \\ \sim \end{bmatrix} \quad (2)$$

where the eigenvalue of ABCD matrix, denoted by  $\lambda$ , can be calculated [12]. Finally, the complex propagation constant, defined by  $\gamma$ , can be obtained by solving Eq. (3).

$$\lambda = e^{\gamma \cdot N \cdot P} \quad (3)$$

In this paper,  $\gamma$  is equal to  $\alpha + j\beta$ , where  $\alpha$  and  $\beta$  are the attenuation and phase constants. The normalized phase constant is equal to  $\beta/\beta_0$ , where  $\beta_0$  is the free space wave number. The normalized attenuation constant is defined by  $\alpha/\beta_0$ .

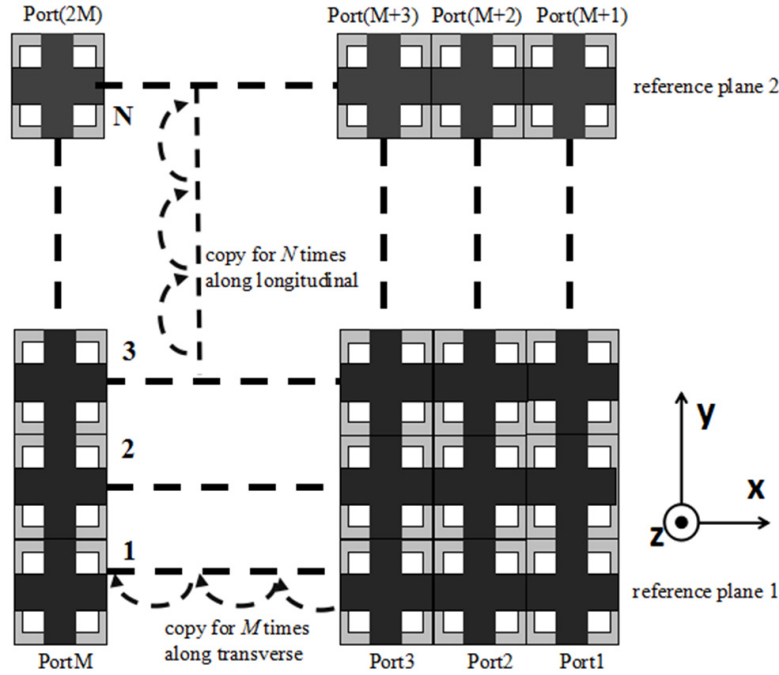


Figure 2. The equivalent multiport network of the perforated microstrip in Fig. 1.

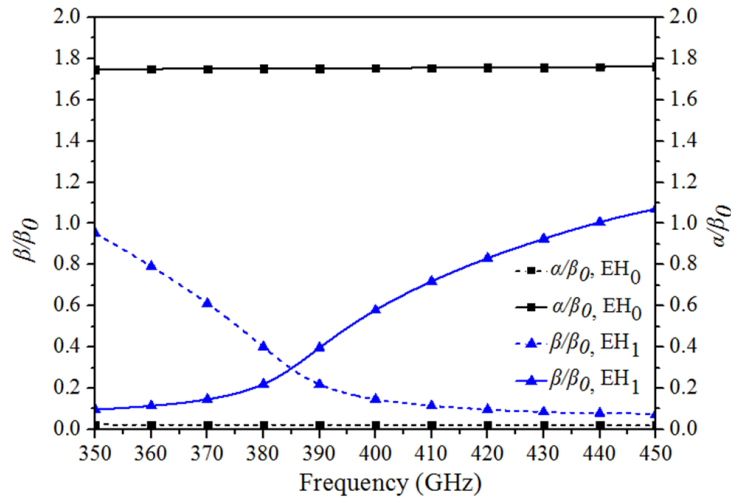


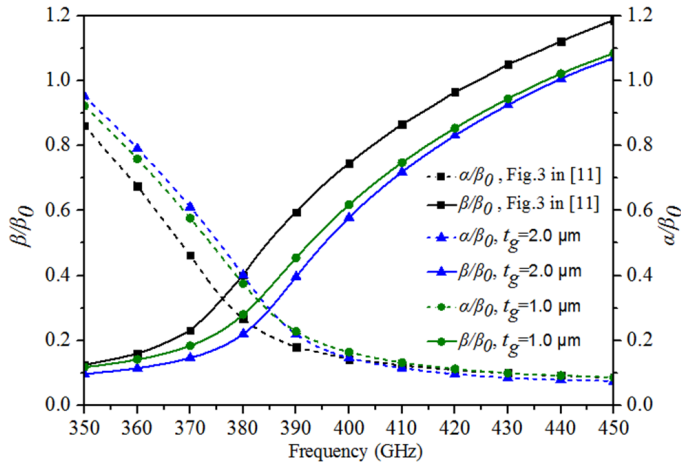
Figure 3. Calculated  $E_{H_0}$  and  $E_{H_1}$  modes of the CMOS perforated microstrip in Fig. 1.

Figure 3 shows the extracted results of the perforated microstrip in Fig. 1. The HFSS simulations are conducted based on the structural and the material parameters summarized in the caption of Fig. 1. The numbers of the unit cell in the transverse and longitudinal directions, denoted by  $M$ , and  $N$  are set as 11 and 20 in this case study. The black and blue curves represent the fundamental ( $E_{H_0}$ ) and first higher order ( $E_{H_1}$ ) modes of the CMOS perforated microstrip in Fig. 1. The slow-wave factor (SWF), equal to the normalized phase constant ( $\beta/\beta_0$ ) of the  $E_{H_0}$  mode is 1.76. The quality factor of the microstrip, equal to  $\beta/2\alpha$ , is 44. The cutoff frequency of the  $E_{H_1}$  mode, defined by the intersecting frequency between the curves of the normalized attenuation and phase constants, is 385 GHz. In the next section, the numerical procedures mentioned above will be applied to improve the unit cell designs for making LWA antenna in high performance.

### 3. UNIT CELL AND FEEDING NETWORK DESIGNS

To design a high performance monolithic leaky wave antenna shown in Fig. 1, a series numerical analyses based on the numerical methods reported in Section 2 are conducted. Fig. 4 shows the analytical results with different unit cell designs. During the analyses, all the widths of the perforated microstrip are identical to  $176\ \mu\text{m}$ . The black curves duplicated the data of Fig. 3 in [11], are also inserted for the comparison. The blue and green curves are the extracted results of the perforated microstrip with a different metal thickness of the ground plane ( $t_g$ ) of the unit cell. The previous cell design in [11], which has  $t_g$  equal to  $2\ \mu\text{m}$ , makes the cutoff frequency of  $\text{EH}_1$  mode at  $376\ \text{GHz}$ , corresponding to normalized attenuation and phase constant equal to  $0.3$ . Based on the unit cell shown in Fig. 1, the cutoff frequency is at  $385\ \text{GHz}$  with  $\alpha/\beta_0$  and  $\beta/\beta_0$  equal to  $0.27$  when  $t_g$  is set as  $2.0\ \mu\text{m}$ . By decreasing  $50\%$  of  $t_g$ , the cutoff frequency can be shifted to  $383\ \text{GHz}$  with  $\alpha/\beta_0$  and  $\beta/\beta_0$  equal to  $0.29$ . Although the thinner metal thickness of the ground plane can generate  $\text{EH}_1$  mode at a lower frequency, the increasing of  $\alpha/\beta_0$  can produce more conductor loss, reducing the antenna gain and efficiency. Similarly, the unique design of the ground plane in [11] can significantly make LWA at a lower frequency without increasing the width of the antenna, but the higher attenuation will reduce the antenna gain. In this paper, the unit cell in Fig. 1, by setting  $t_g$  equal to  $2\ \mu\text{m}$ , can reduce  $14\%$  of the attenuation constant to improve the LWA design.

Additionally, to excite the leaky mode on the perforated microstrip effectively, the on-chip differential feeding network is designed. The feeding network is implemented by using Marchand balun, consisting of two  $90^\circ$   $3\ \text{dB}$  directional couplers. The synthetic coupled-line, so-called the complementary-conducting strip coupled line (CCS-CL) constructs the couplers at  $400\ \text{GHz}$  [13]. By using the design techniques explored in [13], the even and odd mode characteristic impedances of CCS-CL are  $104\ \text{ohm}$  and  $33\ \text{ohm}$ . The slow wave factors (SWF) of even and odd modes are  $1.67$  and  $1.88$ , respectively. Fig. 5 shows the simulated surface currents of the Marchand balun and the antenna at  $400\ \text{GHz}$ , revealing a nearly perfect differential current smoothly injecting into the LWA.



**Figure 4.** Calculated complex propagation constants of the  $\text{EH}_1$  mode in the monolithic perforated microstrip with different unit cell designs.

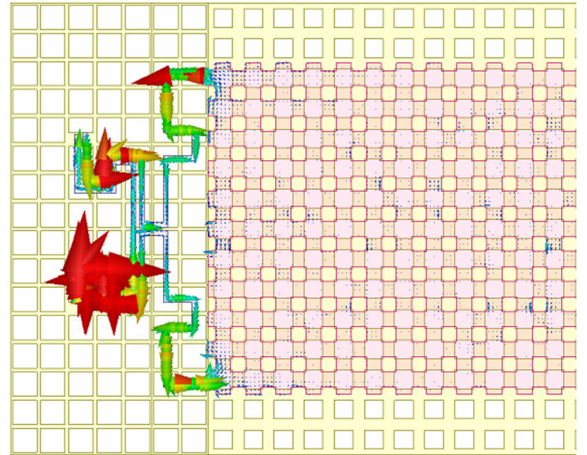


**Figure 5.** Surface current of the differential feeding network and LWA at  $400\ \text{GHz}$ .

### 4. 400 GHz PROTOTYPE AND MEASUREMENTS

Figure 6 shows a chip photo of a  $400\ \text{GHz}$  leaky wave antenna (LWA) in  $0.13\ \mu\text{m}$  CMOS  $1\text{P}8\text{M}$  technology.  $W$  and  $W_h$  of the unit cell in Fig. 1 are equal to  $8$  and  $10\ \mu\text{m}$ , respectively. The prototype is in a chip area of  $0.176\ \text{mm} \times 1.6\ \text{mm}$ , consisting of  $11$  and  $100$  unit cells along the transverse and the longitudinal direction. Based on the blue curves in Fig. 4, the prototype, which has a physical length in  $2.13$  times of the free-space wavelength at  $400\ \text{GHz}$ , can make  $92.3\%$  leakage of the electromagnetic energy.

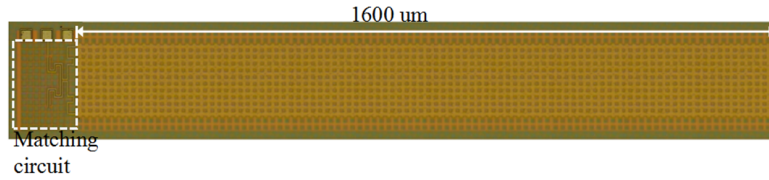


**Figure 6.** A prototype of the 400 GHz monolithic LWA in 0.13 μm CMOS 1P8M process.

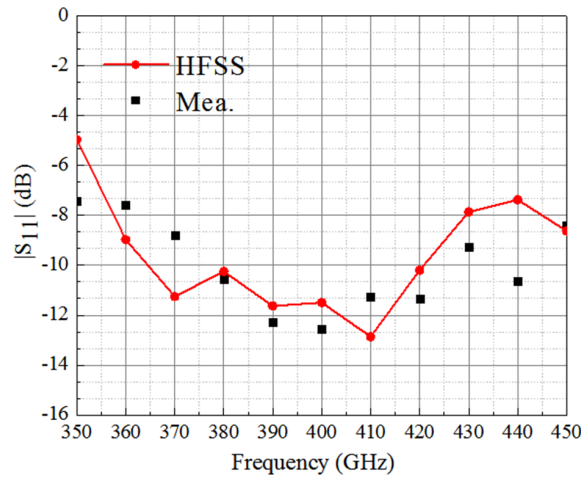


**Figure 7.** Simulated and measured input return loss of the LWA prototype in Fig. 6.

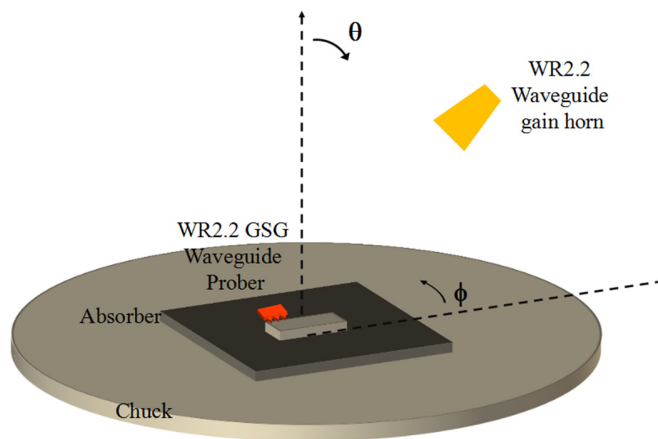


**Figure 8.** Experimental setups of the monolithic LWA at terahertz.

The on-chip matching network, as shown on the left-hand side of the photographic, is in an area of  $80\ \mu\text{m} \times 192\ \mu\text{m}$  to perform the single-end to the differential transformation from the off-chip  $50\ \Omega$  system.

The  $50\ \mu\text{m}$  GSG WR2.2 infinite waveguide probe from Cascade Microtech<sup>TM</sup>, the frequency converter and vector network analyzer of ZVA-Z500, and ZVA40 from Rhode&Schwartz<sup>TM</sup> are calibrated through the one-port SOL (Short-Open-Load) procedures before the on-wafer measurements. The measured input return loss of the CMOS prototype, including the effects of the contact pads, compares with the HFSS simulations. The comparison in Fig. 7, showing the good agreement, reveals both measured and simulated return loss lower than 10 dB from 380 GHz to 420 GHz in the 50-ohm system.

Figure 8 shows the setup for measuring the monolithic LWA at terahertz. The system consists of two ZVA-Z500 frequency converters, one four-port ZVA40 vector network analyzer, and the M150

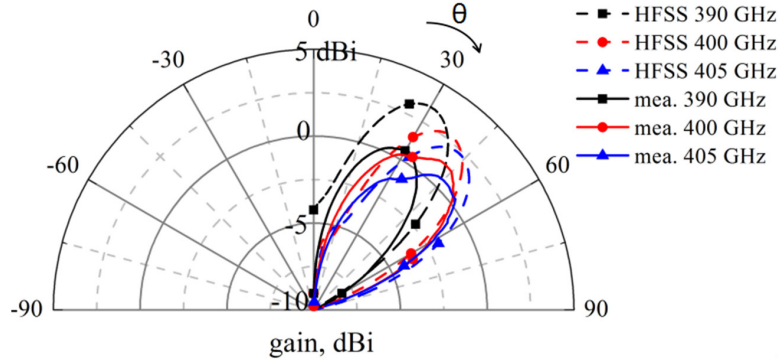


**Figure 9.** Simulated and measured  $H$ -plane radiation patterns of the CMOS prototype at  $\phi = 90^\circ$ .

**Table 1.** Beam scanning of the CMOS prototype.

Frequency	Simu. $\theta$ ( $^\circ$ )	Mea. $\theta$ ( $^\circ$ )	Equation (7)–(39) in [14]	$\beta/\beta_0$
390 GHz	$30^\circ$	$30^\circ$	$23^\circ$	0.396
400 GHz	$38^\circ$	$41^\circ$	$35^\circ$	0.579
405 GHz	$43^\circ$	$45^\circ$	$40^\circ$	0.639
415 GHz	$48^\circ$	$51^\circ$	$51^\circ$	0.778

**Table 2.** Millimeter-wave monolithic integrated antennas.

Ref	Type	Freq (GHz)	Gain (dBi)	Area (mm <sup>2</sup> )
[4]	Log-periodic	94	4.8 (mea.)	$2.6 * 1.2$
[5]	Patch	410	$-1.5$ (sim)	$0.2 * 0.2$
[6]	Metasurface	94	$-2.5$ (mea.)	$2 * 1.3$
[7]	Slotted cavity	140	$-2$ (sim)	$1.2 * 0.6$
[9]	Slotted SIW*	410	$-0.5$ (sim.)	$0.5 * 0.2$
[10]	Dipole	160	$-10$ (sim)	$0.5 * 0.45$
[11]	LWA**	410	$0.4$ (sim.)	$3.2 * 0.17$
This work	LWA**	400	$1.3$ (mea.)	$1.6 * 0.17$

\*:substrate integrated waveguide, \*\*: leaky-wave antenna

probe station from Cascade Microtech<sup>TM</sup>. Two identical 26 dBi WR2.2 diagonal horns from Virginia Diodes<sup>TM</sup> are as the standard gain horns to calibrate the full system. The distance between two gain horns is set as 0.5 meters during the gain calibration. The identical setup, except the GSG waveguide probe, is applied to characterize the LWA prototype in Fig. 6. Due to the mechanical limitation, the scanning angle only covers  $\theta$  from  $0^\circ$  to  $90^\circ$ . The absorber from Cascade Microtech<sup>TM</sup> is inserted between the metal chuck and CMOS prototype to eliminate the diffraction from the environment.

The measured antenna gains, eliminating the losses of the GSG waveguide probe and the contact loss between probe and CMOS pads, are compared with the simulated data. The comparison in Fig. 9 shows the maximum difference of 2.5 dBi between the measured and simulated patterns. This difference may be caused by the absorber near the prototype during the measurements. The solid curves indicate that measured gain is about 0.8 dBi and has a maximum value of 1.3 dBi at 400 GHz. The main beams of the prototype are  $30^\circ$ ,  $42^\circ$ , and  $45^\circ$  from broadside at 390 GHz, 400 GHz, and 405 GHz. The theoretical

calculations, performed by using the equation (7–39) in the textbook [15], show the main beam at  $23^\circ$ ,  $36^\circ$  and  $41^\circ$  from broadside. Table 1 summarizes the calculated results and makes the comparisons with the HFSS simulations and the measurements. The normalized phase constants on the right-hand column I directly copy from the solid blue curve in Fig. 3. The comparisons show good agreements between three validating methods. The measured results in Fig. 9 experimentally prove the numerical procedures in Section 2 and the unit cell design in Section 3.

Table 2 summarizes the reported on-chip antennas in millimeter-wave frequency bands. The log-periodic antenna in [4], realized on a  $100\text{ }\mu\text{m}$ -thickness low-loss GaAs substrate, achieved 4.8 dBi at 94 GHz. The rest of the silicon-based prototypes have the antenna gains below zero dBi. Compared with the design in [11], the LWA in this paper, which is made by a unit cell with the lower material loss, uses the differential feeding network to efficiently excite the leaky mode on the perforated microstrip, experimentally demonstrating the antenna gain of 1.3 dBi at 400 GHz.

## 5. CONCLUSION

A 400 GHz 1.3 dBi monolithic leaky wave antenna (LWA), which is constructed by the unit cell, is presented. The rigorous full-wave eigenvalue method is applied to extract the guiding characteristics of the first higher order mode ( $\text{EH}_1$ ) and further assists in improving the unit cell design. The Marchand balun based feeding network is designed to excite the proposed LWA. A 400 GHz CMOS LWA prototype is designed based on the design curves and experimentally characterized through the on-wafer measurements. The measured antenna gain is higher than 0.8 dBi from 390 GHz to 405 GHz and has a maximum gain of 1.3 dBi at 400 GHz. The measured radiation patterns experimentally confirm the validity of the numerical methods and unit cell design.

## ACKNOWLEDGMENT

The authors wish to extend their sincere thanks to the Silterra Corporation, Malaysia, for providing the chip fabrication. This work was supported in part by the National Natural Science Foundation of China under Grant 61271068 and the Global Expert Program in China.

## REFERENCES

1. Cheema, H. M. and A. Shamim, "The last barrier: on-chip antenna," *IEEE Microw. Mag.*, Vol. 14, No. 1, 79–91, 2003.
2. Chen, I. J., H. Wang, and P. W. Hsu, "A V-band quasi-optical GaAs HEMT monolithic integrated antenna and receiver front end," *IEEE Trans. Microwave Theory Tech.*, Vol. 51, No. 12, 2461–2468, 2003.
3. Abbasi, M., S. Gunnarsson, N. Wadefalk, R. Kozhuharov, J. Svedin, S. Cherednichenko, I. Angelov, I. Kallfass, A. Leuther, and H. Zirath, "Single-chip 220-GHz active heterodyne receiver and transmitter MMICs with on-chip integrated antenna," *IEEE Trans. Microwave Theory Tech.*, Vol. 59, No. 2, 466–478, 2010.
4. Baek, Y. H., L. H. Truong, S. W. Park, S. J. Lee, Y. S. Chae, E. H. Rhee, H. C. Park, and J. K. Rhee, "94-GHz log-periodic antenna on GaAs substrate using air-bridge structure," *IEEE Antennas Wirel. Propag. Lett.* Vol. 8, 909–912, 2005.
5. Seok, E., D. Shim, C. Mao, R. Han, S. Sankaran, C. Cao, W. Knap, and K. O. Kenneth, "Progress and challenges towards terahertz CMOS integrated circuits," *IEEE J. Solid-State Circuits*, Vol. 45, No. 8, 1554–1564, 2008.
6. Pan, S. J., F. Caster, P. Heydari, and F. Capolino, "A 94-GHz extremely thin metasurface-based BiCMOS on-chip antenna," *IEEE Trans. Antennas Propag.*, Vol. 62, No. 9, 4439–4454, 2014.
7. Pan, S. J. and F. Capolino, "Design of a CMOS on-chip slot antenna with extremely flat cavity at 140 GHz," *IEEE Antennas Wirel. Propag. Lett.*, Vol. 10, 827–831, 2011.
8. Bhattacharyya, A. and R. Garg, "Effect of substrate on the efficiency of an arbitrarily shaped microstrip patch antenna," *IEEE Trans. Antennas Propag.*, Vol. 34, No. 10, 1181–1189, 1986.

9. Hu, S., Y. Z. Xiong, B. Zhang, L. Wang, T. G. Lim, M. Je, and M. Madhian, "A SiGe BiCMOS transmitter/receiver chipset with on-chip SIW antennas for terahertz applications," *IEEE J. Solid-State Circuits*, Vol. 47, No. 11, 2654–2665, 2012.
10. Neculoiu, D., A. Muller, E. Laskin, and S. P. Voinigescu, "160 GHz on-chip dipole antenna structure in silicon technology," *Proc. IEEE Int. Semiconductor Conf.*, 245–248, Sinaia, Romania, October 2007.
11. Tzuang, C. K. C., H. S. Wu, X. R. Li, and J. G. Ma, "Monolithic synthetic transmission-line leaky-mode antenna at THz," *The 43rd European Microwave Conf.*, 499–503, Nuremberg, Germany, October, 2013.
12. Li, X. R., C. K. C. Tzuang, and H. S. Wu, "Anomalous dispersion characteristics of periodic substrate integrated waveguides from microwave to terahertz," *IEEE Trans. Microwave Theory Tech.*, Vol. 63, No. 7, 2142–2153, 2015.
13. Tsai, K. H. and C. K. C. Tzuang, "Mode symmetry analysis and design of CMOS synthetic coupled transmission lines," *IEEE MTT-S Int. Microwave Symp.*, 258–262, Boston, MA, 2009.
14. Oliner, A. A. and D. R. Jackson, "Leaky-wave antennas," *Antenna Engineering Handbook*, McGraw-Hill, New York, 2007.